Quantitative Orientation of α-Helical Polypeptides by Attenuated Total Reflection Infrared Spectroscopy

T. Buffeteau,*,† E. Le Calvez,† B. Desbat,† I. Pelletier,‡ and M. Pezolet‡

Laboratoire de Physico-Chimie Moléculaire, UMR 5803 du CNRS, Université Bordeaux I, 33405 Talence, France and Centre de Recherche en Sciences et Ingénierie des Macromolécules, Département de Chimie, Université Laval, Québec, G1K 7P4, Canada

Received: July 26, 2000; In Final Form: November 9, 2000

Spectral simulations of polarized attenuated total reflection (ATR) spectra have been used to quantitatively determine the orientation of α-helical polypeptides. Transmittance and polarized ATR spectra of five monolayers of poly-γ-benzyl-L-glutamate (PBG) transferred by the Langmuir−Blodgett techniques on germanium crystal have been recorded, and the dichroic ratios of the amide I and amide II bands have been calculated. Simulations were performed using anisotropic optical constants of PBG in the molecular coordinate system and using the 4×4 matrix formalism of Berreman. Assuming that the α-helices are parallel to the plane of the ATR crystal, an average angle of $38° \pm 1°$ between the helix axes and the withdrawing direction has been found. Simulated spectra for various orientations of the α-helices are then given and influence of the azimuthal and tilt angles on the dichroic ratios of the amide bands has been investigated.

Introduction

Attenuated total reflection (ATR) infrared spectroscopy is one of the most powerful methods for recording infrared spectra of biological membranes.[1−3] Indeed, it presents several advantages: (i) information about molecular conformation can be obtained from the position, the shape, and the intensity of the observed bands; (ii) information about molecular orientation can be obtained from measurements with polarized light; (iii) ATR spectra with a good signal-to-noise (S/N) ratio require only few micrograms of sample; (iv) lipids and peptides can be easily supported on ATR crystals; and (v) experiments can be made in an aqueous environment. ATR spectroscopy has thus been used extensively to study phospholipid monolayers and multilayers,[3−10] polypeptides or proteins,[1−3,11−13] and lipid−proteins complexes.[1−3,14−21] Thin films of phospholipids (with or without proteins) can be prepared using different techniques: (i) monolayers can be deposited onto the ATR crystal by Langmuir−Blodgett (LB) technique;[16,19−22] (ii) single supported bilayers can be obtained by spontaneous adsorption and fusion of small unilamellar vesicles on phospholipid monolayers deposited by LB technique;[9,17,18] (iii) multibilayers can be formed by evaporation from organic solvent.[3,13,15,21]

In polarized ATR studies, the molecular order parameter is normally calculated in three steps.[3,13] First, the dichroic ratio R_{ATR} for a selected vibrational mode is determined by calculating the ratio of the absorbance measured with the infrared radiation polarized parallel (p) and perpendicular (s) to the plane of incidence ($R_{ATR} = A_p/A_s$). Second, assuming a uniaxial distribution of orientation of the molecules with respect to the normal to the ATR crystal (*z* axis), the order parameter S_z is calculated for the transition dipole moment **M** of the selected mode using the following equation[3]

$$S_z = \frac{\langle E_x^2\rangle - \langle E_y^2\rangle \cdot R_{ATR} + \langle E_z^2\rangle}{\langle E_x^2\rangle - \langle E_y^2\rangle \cdot R_{ATR} - 2 \cdot \langle E_z^2\rangle} \quad (1)$$

where $\langle E_x^2\rangle$, $\langle E_y^2\rangle$, and $\langle E_z^2\rangle$ are the mean square electric field (MSEF) amplitudes of the evanescent polarized radiation in the film. The MSEF amplitudes can be calculated approximately using Harrick equations for thick nonabsorbing films (film thickness very large compared to the penetration depth of the evanescent wave),[23] and for ultrathin films (film thickness lower than 100 Å),[24] or exactly using thickness- and absorption-dependent equations.[25,26] Third, assuming a cylindrical symmetry of the molecules with respect to the molecular axis *w*, the molecular order parameter $S_m = \langle P_2(\cos\gamma)\rangle$ can be calculated from the order parameter of the transition dipole moment S_z, using the Legendre addition theorem

$$S_m = \frac{3 \cdot \langle \cos^2\gamma\rangle - 1}{2} = \frac{S_z}{\langle P_2(\cos\beta)\rangle} \quad (2)$$

where γ is the angle between the molecular axis and the normal to the ATR crystal, and β is the angle between the transition moment and the molecular axis (see Figure 1). The angle β is generally considered as fixed, that is, the orientation distribution of the transition moment about the molecular axis is infinitely narrow, so that $\langle P_2(\cos\beta)\rangle = P_2(\cos\beta)$. The molecular order parameter S_m ranges from 1.0 for $\gamma = 0°$ (all the molecular axes are aligned parallel to the *z* axis) to −0.5 for $\gamma = 90°$ (all the molecular axes are aligned perpendicular to the *z* axis). For other values of S_m, the molecular orientation can be described by a distribution function or by a single angle γ (if the distribution function is infinitely narrow) given by the relation

$$\gamma = \arccos\sqrt{\frac{2 \cdot S_m + 1}{3}} \quad (3)$$

* To whom correspondence should be addressed. E-mail: thbuff@lpct.u-bordeaux.fr. Fax: (33) 5 56 84 84 02.

† Laboratoire de Physico-Chimie Moléculaire, UMR 5803 du CNRS, Université Bordeaux I.

‡ Centre de Recherche en Sciences et Ingénierie des Macromolécules, Département de Chimie, Université Laval.

10.1021/jp002655s CCC: $20.00
Published on Web 01/26/2001

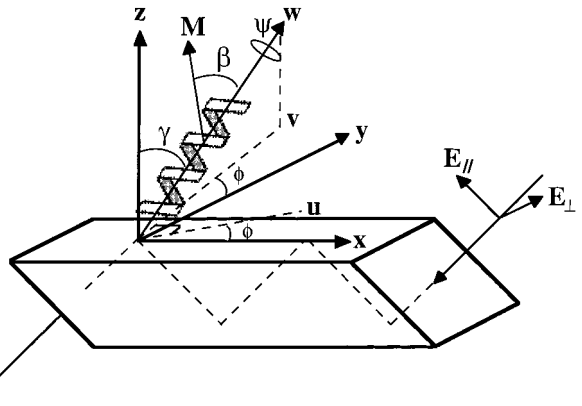

Figure 1. Coordinate and angle conventions used in the current investigation. The (*x*,*y*) plane is parallel to the germanium crystal surface, and the (*x*,*z*) plane is parallel to the plane of incidence. γ is the angle between the helix axis (*w* axis) and the *z* axis. β is the angle between the selected transition diople moment and helix axis. ϕ is the azimuthal angle of the helix axis. (*u*, *v*, *w*) represent the molecular axes after rotation of the azimuthal and tilt angles. The withdrawing direction is along the *y* axis.

For example, for the special case of $S_m = 0$, the orientation could be interpreted as an isotropic distribution of the molecular axes or as a delta distribution centered at $\gamma = 54°.7$.

Although polarized ATR spectroscopy provides valuable information about the molecular orientation, its quantitative approach presents some limitations. The first limitation involves the determination of both the MSEF and the refractive indexes of the system. Indeed, there are significant differences in the manner to estimate the MSEF amplitudes of the evanescent polarized radiation in ultrathin films. Generally, Harrick thin film approximation is used to calculate MSEF amplitudes, assuming that the film is thin enough so that there is no significant change of the MSEF amplitudes over the film thickness. The Harrick equations has been used successfully by most investigators studying thin membrane samples. However, Citra et al.[13] have recently proposed that for very thin films, the optical constants of the film are highly perturbed by the optical properties of the adjacent media and that the optical properties of the film should be neglected. This model, named the two-phase approximation, has also been used in the literature by other investigators.[11,12,27,28] In addition, whatever the model used, the knowledge of the refractive index of the different layers (crystal, film, and environment) is important to calculate accurately the MSEF amplitudes in the film. The refractive index of the ATR crystals is well-known ($n = 4.0$ for germanium, $n = 3.42$ for silicon, $n = 2.43$ for zinc selenide, and $n = 2.38$ for KRS5).[29,30] Likewise, the complex refractive indexes of the H_2O and D_2O environment have been determined by Bertie et al.[31,32] In contrast, very few information concerning the complex refractive indexes of lipid membranes and proteins are found in the literature. Refractive indexes of about 1.4−1.5 are used in the mid infrared for lipid membranes,[3] whereas for lipid−protein complexes, the range of values reported in the literature is larger (1.35−1.7).[17,33−36] Generally, in all polarized ATR studies, the extinction coefficient of the film is neglected in the calculation of the MSEF amplitudes, considering that lipid membranes and proteins are weakly absorbent in the spectral range of interest. A second limitation concerns the knowledge of the orientation of the transition moment of the selected mode with respect to the molecular axis, which is required to precisely compute the molecular order parameter using eq 2. The dipole orientation is well-defined in phospholipids if the acyl chains are in the all-trans conformation ($\beta = 90°$ for the $\nu_a CH_2$ and $\nu_s CH_2$ vibrations and $\beta = 0°$ for the wagging band progression).[2,3] In contrast, for polypeptides and proteins with α-helical secondary structure, the dipole orientation of the amide I and amide II modes is more controversial. Indeed, values of the β angle reported in the literature vary between 24° and 40° for the amide I mode and between 73° and 88° for the amide II mode.[33,37−42] In addition, for some conformations, such as β-sheets, the transition moments do not exhibit a cylindrical symmetry along the molecular axis. In such a case, Marsh has shown that the quantitative evaluation of the molecular orientation requires the measurement of the dichroic ratio of two bands with orthogonal transition moments.[43] Finally, the simple approach given above does not apply for systems in which the orientation distribution is not uniaxial. For such a case, Ahn and Franses have expressed the dichroic ratio in terms of the azimuthal and tilt angles for particular values of the β angle.[44,45] Since several combinations of the azimuthal and tilt angles are solution of a given value of the dichroic ratio, it is necessary to perform two experiments to determine the acceptable solution. Practically, either ATR dichroic ratios are measured for two orientations of the ATR plate,[44] or polarized ATR and transmittance spectra are recorded using the same sample.[45]

These limitations can be overcome by determining from polarized transmittance and reflectance infrared spectra the anisotropic optical constants (index of refraction *n* and extinction coefficient k) of oriented thin films. In addition to providing the wavenumber dependence of the complex refractive indexes, this approach allows the calculation of the average orientation of each transition moment and of the molecules when their conformation is known.[46,47] Furthermore, the anisotropic optical constants allow the simulation of transmittance and reflectance infrared spectra under various experimental conditions (incidence angle, polarization parallel or perpendicular to the plane of incidence) of thin films deposited onto different substrates. For example, this approach is particularly valuable to simulate polarized ATR spectra of thin films of polypeptides for different tilt angles of α-helices or β-sheets with respect to the surface normal in a uniaxial orientation model. Moreover, spectral simulations for different azimuthal angles of the secondary structures provide quantitative information on the in-plane orientation anisotropy for nonuniaxial systems. From these simulated spectra, plots of the dichroic ratio versus tilt or azimuthal angles of the molecular axis can be obtained for selected bands. In this quantitative approach of the molecular orientation, it is not necessary to know the MSEF amplitudes of the polarized light in the film and the orientation of the transition dipole moment of the selected bands. Moreover, the wavenumber dependence of the refractive index and of the extinction coefficient of the film is taken into account. This method has been applied for a quantitative molecular orientation in thin lipid films.[48]

Recently, the anisotropic optical constants of thin LB films of the α-helical polypeptide poly-γ-benzyl-L-glutamate (PBG) have been determined in the mid-infrared.[49] This study has shown that the PBG α-helices are oriented parallel to the surface with a preferential orientation of the helix axis along the withdrawing direction. From these anisotropic optical constants, the angles between the transition moments of the amide vibrations and the helix axis have been determined, and the values obtained are in very good agreement with those recently published by Marsh et al.[42] Furthermore, the PM-IRRAS spectrum of a monolayer at the air/water interface was simulated satisfactorily. In the current study, the anisotropic optical constants of PBG have been used to simulate polarized ATR

spectra. These spectra have been compared with those obtained experimentally for thin LB films to validate the optical constants. Moreover, spectral simulations have also been performed to show the effect of the tilt and azimuthal angles of the α-helices on the polarized ATR spectra.

Materials and Methods

Materials. PBG (molecular weight 22 000 (vis)) and HPLC grade chloroform were purchased from Sigma-Aldrich and used without any further purification. The subphase was prepared with deionized water with a resistivity of 18.3 MΩ/cm (Barnstead Nanopur II, Boston, MA).

Formation and Deposition of LB Films. The monolayer experiments were performed with a KSV-3000 Langmuir film balance apparatus (KSV Instruments, Helsinki, Finland). The Teflon trough (15 × 49 × 1.5 cm) was thoroughly cleaned and then filled with pure deionized water. The temperature was fixed at 17 ± 1 °C. ATR germanium parallelogram crystals (50 × 20 × 2 mm with a 45° face angle, 24 internal reflections) were used as substrates for the deposition of the films. They were cleaned with chloroform in a bath sonicator for 5 min, rinsed with chloroform, and finally put in a plasma cleaner (Harrick Scientific, Ossining, NY) for 2 min. The crystals were then lowered into the subphase at a depth of 10 mm and 75 μL of PBG solution (1 mg/mL in chloroform) were spread onto the subphase. After an equilibration period of 15 min, allowing solvent evaporation, the surface area of the bath was lowered at a rate of 90 cm^2/min. The evolution of the surface pressure was monitored by the Wilhelmy method using a platinum plate. The surface pressure−area isotherm was very similar to those obtained previously by others for PBG.[11,50−52]

To transfer the first monolayer on the substrate, the film was compressed at a surface pressure of 5 mN/m corresponding to a molecular area of 18.5 Å^2/monomer and held at this pressure for 20 min. The substrate was then raised at a rate of 2.0 mm/min with its large face horizontal. The transfer ratio was equal to 0.95 ± 0.05. After deposition of the first layer, the film was allowed to dry for 2 h and was then immersed in the subphase at a rate of 10 mm/min to transfer the second layer. For the transfer of the remaining layers (up to 5), the same procedure was used but the drying time was only 1 h.

FTIR Measurements. Infrared spectra were recorded with a Magna 750 Fourier transform infrared spectrometer (Nicolet Instrument, Madison, WI) equipped with a narrow-band liquid nitrogen cooled mercury−cadmium−telluride detector. The spectrometer was continuously purged with dry air. To obtain the ATR spectra, the germanium crystals were placed in a vertical ATR accessory (Harrick Scientific, Ossining, NY). A motorized rotating ZnSe wire-grid polarizer (Specac, Orpington, UK) positioned in front of the ATR unit was used to obtain polarized spectra without breaking the purge of the spectrometer. Polarized transmittance experiments were also performed at normal incidence to obtain the infrared spectra of PBG thin films in the substrate plane (parallel or perpendicular to the withdrawing direction). For the ATR and transmittance spectra, 250 scans and 1000 scans at 4 cm^{-1} resolution were co-added, respectively. For all measurements, reference spectra of the bare germanium crystals were recorded immediately after those of the transferred monolayers. Experiments were reproduced at least three times, and the reported data represent average values from these experiments. Dichroic ratios were determined from the peak heights of the amide I and amide II bands. All data manipulations were performed with Grams 32 software (Galactic Industries, Salem, NH).

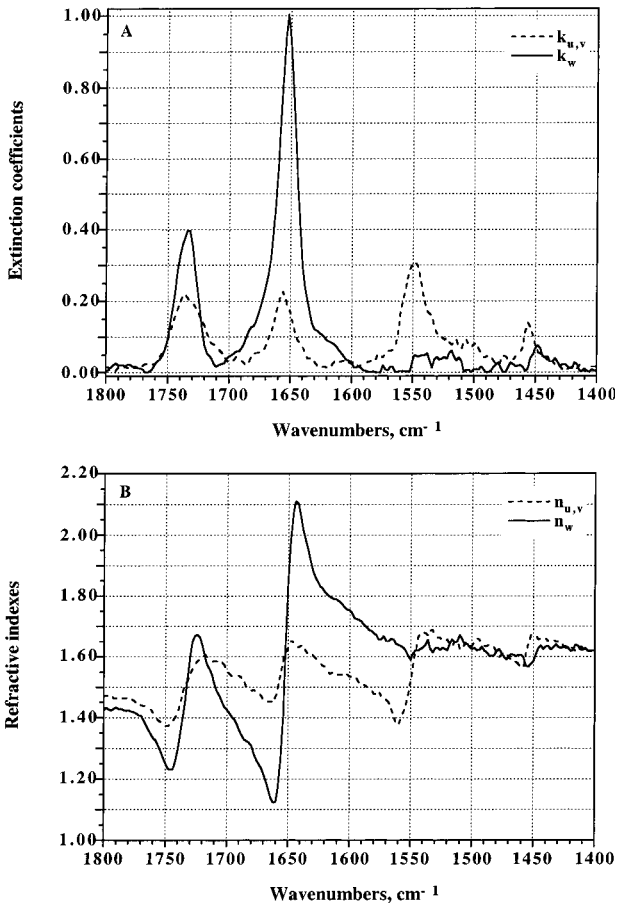

Figure 2. (A) Anisotropic extinction coefficients ($k_{u,v}$ and k_w) and (B) refractive indexes ($n_{u,v}$ and n_w) in the molecular coordinate system of PBG monolayer.

Determination of the Optical Constants of PBG. The anisotropic optical constants of a poly-γ-benzyl-L-glutamate monolayer have recently been determined.[49] First, the optical constants along the *x*, *y*, and *z* directions of the substrate (space coordinate system) were calculated using an iterative procedure based on the inversion of spectral simulation programs.[46] In this procedure, the in-plane (*x* and *y*) and out-of-plane (*z*) refractive indexes were obtained from polarized normalized transmittance spectra at normal incidence and a parallel polarized reflectance spectrum at grazing incidence (IRRAS), respectively. Then, the determination of the anisotropic optical constants in the molecular coordinate system has been performed considering both the orientation of the α-helices on the surface ($\gamma = 90°$ for PBG monolayer) and the symmetry of the α-helices (uniaxial symmetry along the helix axis). The values obtained for the extinction coefficients perpendicular, $k_{u,v}$, and along, k_w, the helix axis are shown in Figure 2a. The refractive indexes in the molecular coordinate system (Figure 2b) have been calculated by Kramers−Kronig transformations of the corresponding extinction coefficients, using a value of n_∞ (index of refraction in the visible) of 1.55.

Simulation of Polarized ATR Spectra. The polarized ATR spectra of PBG thin films deposited onto a germanium crystal have been calculated, for different orientations of the α-helices, using the 4 × 4 matrix formalism of Berreman.[53,54] In this formalism, each layer of a multilayer system can be characterized by a 6 × 6 optical matrix which can be conveniently partitioned as follows

$$\mathbf{M} = \begin{pmatrix} \epsilon & \rho \\ \rho' & \mu \end{pmatrix} \quad (4)$$

where $\epsilon = n^2 = (M_{ij})$ and $\mu = (M_{i+3,j+3})$, $i, j = 1, 2, 3$ are the dielectric and permeability tensors, respectively, and $\rho = (M_{i,j+3})$ and $\rho' = (M_{i+3,j})$, $i, j = 1, 2, 3$ are optical-rotation tensors. In our case, the optical-rotation tensors are null matrix and the permeability tensor is the identity matrix. The orientation of the α-helices has been described by the Euler's angles ϕ (azimuthal angle, rotation around z), γ (tilt angle, rotation around u) and ψ (twist angle, rotation around w) with respect to the fixed *xyz* coordinate system (Figure 1). The dielectric tensor has been calculated for each orientation of the α-helices by the relation

$$\epsilon = \mathbf{A}\begin{pmatrix} \epsilon_{u,v} & 0 & 0 \\ 0 & \epsilon_{u,v} & 0 \\ 0 & 0 & \epsilon_{w} \end{pmatrix}\mathbf{A}^{-1} \quad (5)$$

where $\epsilon_{u,v}$, ϵ_w are the principal dielectric constants of the α-helices and *A* is the coordinate rotation matrix given by[55]

$$\mathbf{A} = \begin{pmatrix} \cos\psi\cos\phi - \cos\gamma\sin\phi\sin\psi & -\sin\psi\cos\phi - \cos\gamma\sin\phi\cos\psi & \sin\gamma\sin\phi \\ \cos\psi\sin\phi + \cos\gamma\cos\phi\sin\psi & -\sin\psi\sin\phi + \cos\gamma\cos\phi\cos\psi & -\sin\gamma\cos\phi \\ \sin\gamma\sin\psi & \sin\gamma\cos\psi & \cos\gamma \end{pmatrix} \quad (6)$$

Then, the 4 × 4 differential propagation matrix Δ of each layer is calculated from the elements of the corresponding optical matrix **M**. General formulas for the components of Δ are given by Berreman[53] or Azzam and Bashara.[54] The following step consists of determining the 4 × 4 layer matrix $\mathbf{L}_j(d_j) = e^{-i\omega d_j \Delta_j}$ that relates the generalized field vector $\psi = (E_x, H_y, E_y, -H_x)$ at upper and lower sides of the *j*th layer. In some simple cases, the matrix layer $\mathbf{L}_j(d_j)$ can be calculated analytically (when Δ^n has a closed-form expression), but generally, it must be calculated numerically (diagonalization of the differential propagation matrix to determine the four eigenvalues and the corresponding eigenvectors). Finally, the 4 × 4 transfer matrix **L** that relates the generalized field vectors at the first and the final boundary of the multilayer system are given by

$$\psi(d = d_1 + d_2 + ...d_N) = \prod_{j=1}^{N-1}\mathbf{L}_j \cdot \psi(0) = \mathbf{L}\cdot\psi(0) \quad (7)$$

The polarized reflection and transmission coefficients can be obtained with the use of the components of the transfer matrix **L**.[53,54]

ATR spectra have been simulated considering the first phase as the denser medium, the second phase as the PBG thin film with a thickness of 15 Å per monolayer, and the last phase as the environment (air). ATR spectra have been simulated for a germanium crystal (i.e., index of refraction $n = 4$), using an angle of incidence of 45°. Polarized ATR spectra (R_p or R_s) are calculated for 24 reflections in the crystal and are normalized by the ATR spectra calculated without PBG thin film ($R_p(0)$ or $R_s(0)$). These simulated ATR spectra are represented in absorbance ($-\log(R_p/R_p(0))$ or $-\log(R_s/R_s(0))$).

Results and Discussion

Polarized Transmittance of a LB Multilayer of PBG. Previous results have shown that LB multilayers of PBG deposited onto CaF_2 substrate present anisotropy in the plane of the film with a preferential orientation of the helix axes along the withdrawing direction.[49] To check if such an anisotropy of orientation also occurs when PBG is transferred onto germanium, polarized transmission measurements were first performed. Figure 3 shows the absorbance spectra between 1800 and 1400 cm^{-1} of five monolayers of PBG deposited on each side of a germanium ATR crystal. These spectra were obtained with the incident light polarized parallel (*y* axis) and perpendicular (*x* axis) to the withdrawing direction. The main bands in these spectra at 1732, 1652, and 1549 cm^{-1} are assigned to the ester C═O stretching vibration of the side chain, the amide I and amide II modes, respectively. The observed position and shape of both the amide I and amide II bands reveal that the conformation of the polypeptide chain in the monolayers is highly α-helical.[37,56] As can be seen, a significant dichroism is observed for the amide I and amide II bands, showing that the helix axes are also preferentially oriented along the withdrawing direction when germanium is used as a substrate. Values of the dichroic ratio, R_T, for the amide I and amide II bands are given in Table 1. To obtain quantitative information about this in-plane anisotropy, spectral simulations were carried out using the anisotropic optical constants of PBG (Figure 2). These simulations were performed assuming that the α-helices are parallel to the plane of the film ($\gamma = 90°$) and by varying the azimuthal ϕ angle. It is noteworthy that for such an orientation of the α-helices, the azimuthal angle ϕ (used in the rotation matrix, eq 6) corresponds to the angle between the helix axis and the withdrawing direction (*y*). To reproduce the experimental dichroic ratio of both the amide I and II bands, an average azimuthal angle between the helix axes and the withdrawing direction of 38 ± 1° has been found, in agreement with previous results for PBG on other substrates.[11,49]

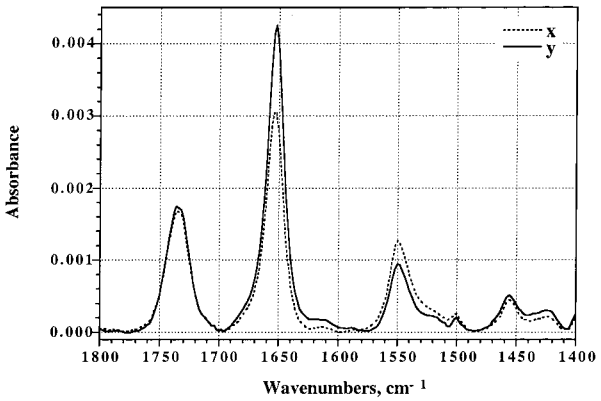

Figure 3. Absorbance spectra of five monolayers of PBG deposited on each side of a germanium ATR crystal, with the incident light polarized parallel (solid line) and perpendicular (dashed line) to the withdrawing direction.

TABLE 1: Dichroic Ratios of the Amide I and Amide II Bands of PBG Calculated from Transmission (R_T) and ATR (R_{ATR}) Experiments

mode (cm^{-1})	R_T[a]	R_{ATR}[a]
amide I (1652)	0.70 ±0.02	0.69 ± 0.02
amide II (1549)	1.34 ± 0.04	1.83 ± 0.05

[a] Averages from three experiments.

Polarized ATR of a LB Multilayer of PBG. Experimental p and s-polarized ATR spectra between 1800 and 1400 cm^{-1} of the same PBG sample used for the transmission measurements are shown in Figure 4a and 4b, respectively. As expected, an important dichroism is also observed for these ATR spectra. Values of the dichroic ratio, R_{ATR}, for the amide I and amide II bands are given in Table 1. Using the azimuthal angle of 38° obtained from the transmission measurements and the aniso-

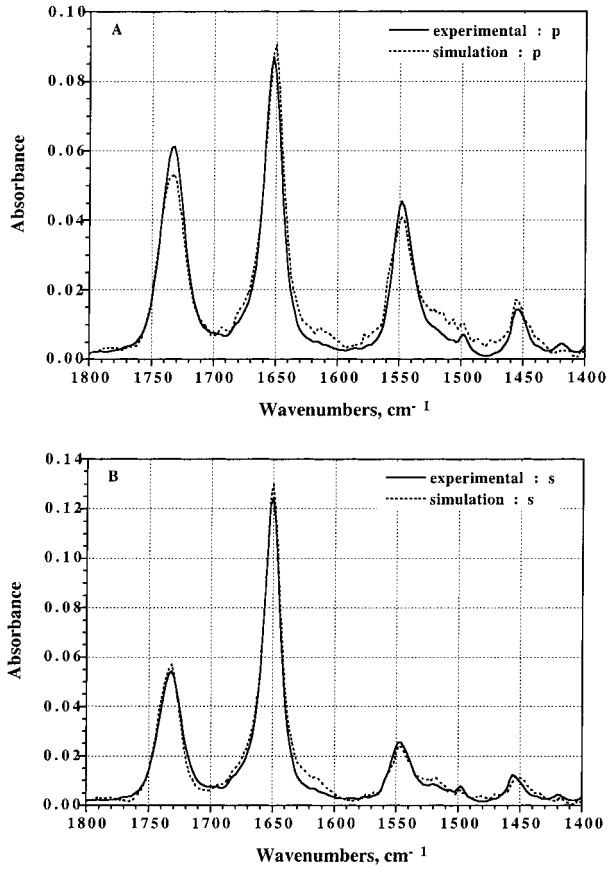

Figure 4. Experimental and simulated ATR spectra of five monolayers of PBG deposited on each side of a germanium crystal, for (A) p and (B) s polarization of the infrared radiation.

tropic optical constants of PBG, the p and s-polarized ATR spectra were calculated. These calculated spectra have been multiplied by 24 to take into account the multiple reflections inside the germanium ATR crystal. As seen in Figure 4, the agreement between the experimental and simulated spectra is very good, showing that the anisotropic optical constants obtained with PBG monolayers transferred on CaF_2 and gold substrates[49] are also valid for PBG on germanium. Furthermore, this agreement also demonstrates that the approach used based on the optical properties of multilayer systems is highly efficient to simulate ATR spectra of uniaxial and nonuniaxial systems and to determine quantitatively the average molecular orientation in these systems. Finally, these results also show clearly that the optical properties of the thin peptide film have to be taken into account, as opposed to the two-phase model proposed by Citra et al.[13]

Influence of the Azimuthal Angle ϕ on Polarized ATR Spectra. One of the major advantages of using the anisotropic optical constants to calculate infrared spectra is that it is easy to simulate the expected spectra for various orientations and symmetry of the molecular axes. For example, Figure 5 shows the effect of the azimuthal angle between the helix axis and the withdrawing direction on the simulated p- and s-polarized ATR spectra of PBG. The simulated spectra were calculated using model optical constants (considering only the amide I and amide II modes) obtained from the experimental anisotropic optical constants of PBG, using a curve-fitting procedure. Component band shapes with a 90%:10% sum of Lorentzian and Gaussian contributions were used. The parameters (frequency, half-width at half-height, and height) obtained from the fit of the amide I and amide II components (perpendicular and along the helix

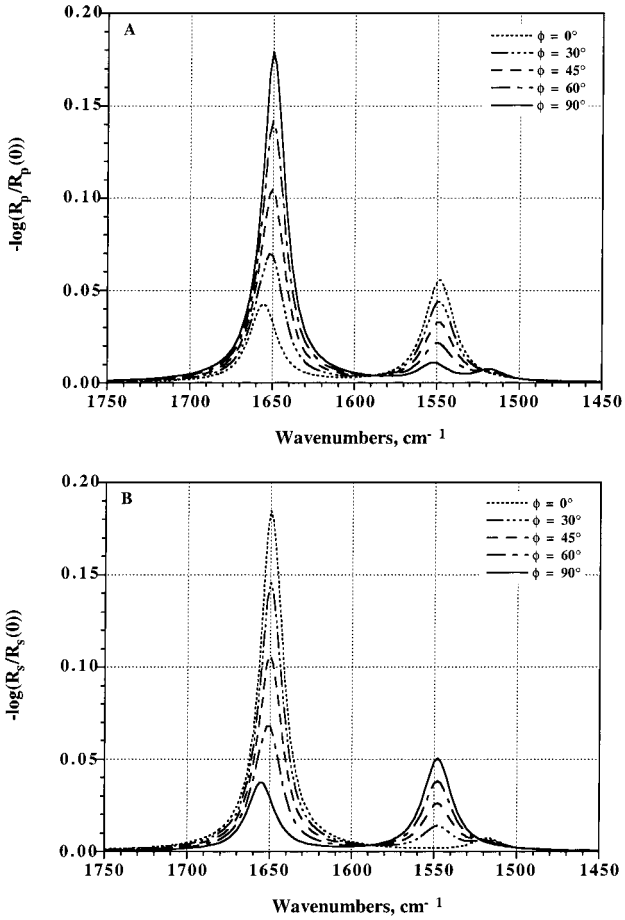

Figure 5. Simulated normalized (A) p- and (B) s-polarized ATR spectra ($-\log(R_p/R_p(0))$ and $-\log(R_s/R_s(0))$) of germanium/PBG/air system for different azimuthal angles $\phi = 0°$, 30°, 45°, 60°, and 90°. Simulations were performed for five monolayers of PBG, assuming that all the helices are parallel to the germanium surface.

TABLE 2: Position, Height, and Half-Width at Half-Height (HWHH) of the Amide I and Amide II Components Used to Calculate Model Anisotropic Extinction Coefficients of PBG

direction	component	position (cm^{-1})	HWHH (cm^{-1})	height
u,*v*	amide I	1656	19.7	0.22
	amide II	1549	21.0	0.305
w	amide I	1652	18.4	1.0
	amide II	1518	21.0	0.04

axis) are given in Table 2. Simulations were performed for five monolayers of PBG, assuming that all α-helices are parallel with respect to the germanium surface (i.e., $\gamma = 90°$).

Figure 5, parts a and b, shows that the intensity of the amide I and amide II bands and their ratio are very sensitive to the azimuthal angle and to the polarization of the infrared radiation. For p-polarized spectra, the intensity of the amide I band increases when the azimuthal angle increases, whereas an inverse behavior is observed for the amide II band. Conversely, for s-polarized spectra, the intensity of the amide I band decreases when the azimuthal angle increases while that of the amide II band increases. The position of the amide I band shifts by about 6 cm^{-1} when the helix axis is either along the *y* direction ($\phi = 0°$) for the p-polarization or along the *x* direction ($\phi = 90°$) for the s-polarization. This result comes from the fact that, for both cases, the perpendicular component (u,v direction) of the amide I band is excited by the electric field. It is well-known that the coupling between the amide vibrations within the α-helix repeat unit results in the splitting of both the amide I and amide II vibrations in two components, one along the helix axis

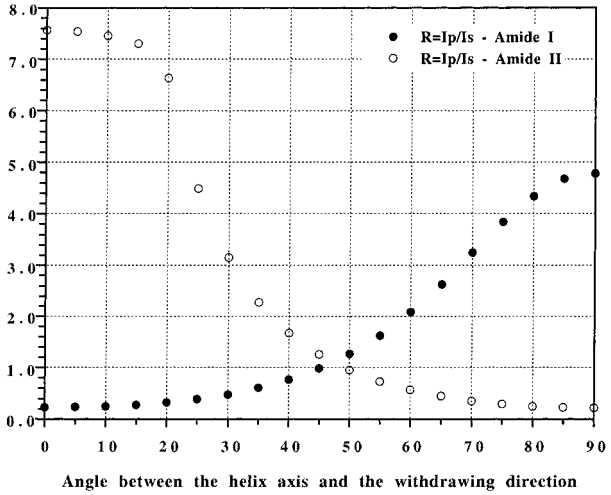

Figure 6. Influence of the azimuthal angle on the dichroic ratios of the amide I and amide II bands.

(*w* direction) with A symmetry and one perpendicular to the helix axis (u,v direction) with E symmetry.[42,56] Since the perpendicular component is located at a higher wavenumber than the parallel one (*w* direction),[56] the amide I band is observed at higher frequency when the electric field is perpendicular to the helix axis. The amide II mode is observed at 1549 cm^{-1} in the calculations, except when the parallel component of the amide II vibration (at 1518 cm^{-1}) is excited by the electric field. This case happens for s polarization when the helix axes are along *y* direction. These observation are in excellent agreement with the spectra recently published by Marsh et al.[42] on highly oriented polyglutamate copolymers.

From these polarized spectra, we have calculated the dichroic ratios of the amide I and amide II bands at the maximum intensity for the different azimuthal angles of the α-helices and their dependence is presented in Figure 6. The dichroic ratio of the amide I band increases from 0.23 when the α-helices are along *y* direction ($\phi = 0°$) to 4.78 when the α-helices are along *x* direction ($\phi = 90°$). Conversely, the dichroic ratio of the amide II band decreases from 7.57 to 0.22 when the azimuthal angle ϕ increases from 0° to 90°. The values of the dichroic ratio calculated from the experimental spectra (Table 1) are consistent with the azimuthal angle of 38° ± 1° calculated from the polarized transmission experiments. Finally, these calculations show that, if a uniaxial orientation model of the α-helices (i.e., $\phi = 45°$) is considered, dichroic ratios of 0.98 and 1.25 are expected for the amide I and amide II bands, respectively. Dichroic ratios close to these values have been found ($R_{ATR} = 0.95 \pm 0.02$ and $R_{ATR} = 1.29 \pm 0.04$ for the amide I and amide II bands, respectively) when only one monolayer is deposited onto the germanium crystal (unshown results).

Influence of the Tilt Angle γ on Polarized ATR Spectra. In this section, polarized ATR spectra have been calculated for different tilt angles γ of the α-helices. Simulations were performed for five monolayers of PBG. The simulated spectra were calculated considering a uniaxial orientation of the α-helices with respect to the normal of the substrate surface (i.e., $\phi = 45°$) and keeping constant the monolayer thickness (15 Å).

Figure 7,a and b, show the normalized p- and s-polarized ATR spectra of PBG, respectively, for different tilt angles from 0° to 90°. As can be seen, the intensity of the amide I and amide II bands and their ratio are also very sensitive to the orientation of the α-helices. For the two polarizations, the intensity of the amide I band increases when the tilt angle increases, whereas

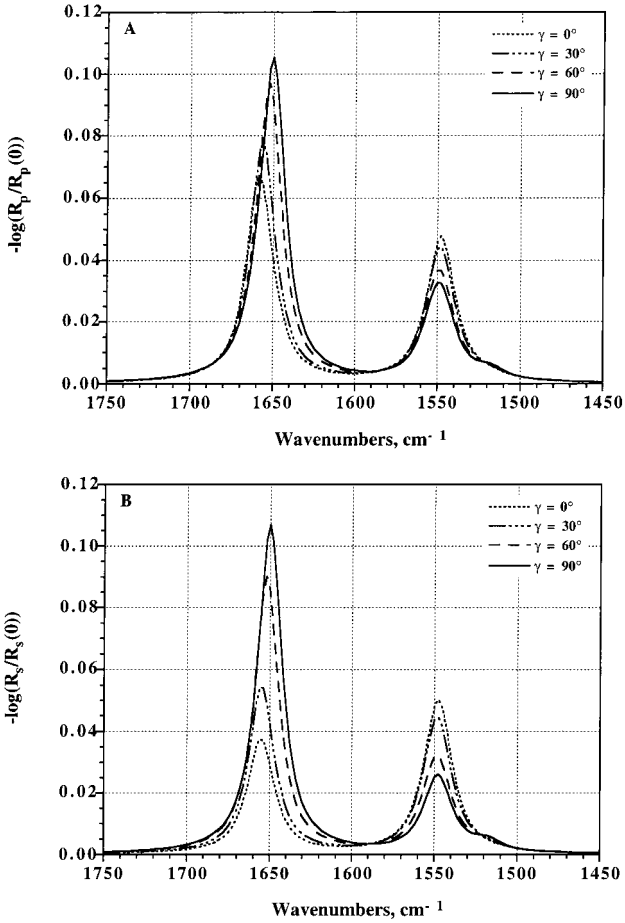

Figure 7. Simulated normalized (A) p- and (B) s-polarized ATR spectra ($-\log(R_p/R_p(0))$ and $-\log(R_s/R_s(0))$) of germanium/PBG/air system for different tilt angles $\gamma = 0°$, 30°, 60°, and 90°. Simulations were performed for five monolayers of PBG, assuming a uniaxial orientation of the helices with respect to the normal of the germanium surface.

an inverse behavior is observed for the amide II band. These intensity changes are more pronounced for the polarization perpendicular to the plane of incidence. Figure 7 also shows that the position of the amide I band is dependent on the tilt angle γ. Indeed, the wavenumber of the amide I band increases when the α-helices are normal to the germanium surface. This frequency shift is slightly more pronounced for the p-polarization (~8 cm^{-1}) than for the s-polarization (~6 cm^{-1}) and can be mainly explained by the fact that the amide I perpendicular component along the u,v direction is preferentially excited by the electric field. On the other hand, the amide II band is located at 1549 cm^{-1}, independently of the tilt angle and the polarization of the light.

The dichroic ratios of the amide I and amide II bands are plotted in Figure 8 as a function of the tilt angle. The dichroic ratio of the amide I band increases from 0.98 when the α-helices are parallel to the crystal surface ($\gamma = 90°$) to 1.80 for a perpendicular orientation of the helix axes ($\gamma = 0°$). Conversely, the dichroic ratio of the amide II band decreases from 1.25 to 0.95 when the tilt angle γ decreases from 90° to 0°. Nevertheless, the dichroic ratios of the two modes vary only slightly for tilt angles between 60° and 90°. The value of the dichroic ratio expected for isotropic distribution ($\gamma = 54.7°$) is the same for the two modes ($R_{ATR}^{iso} = 1.10$). It is noteworthy that the R_{ATR}^{iso} expression used from the MSEF amplitudes[1,24] (i.e., $R_{ATR}^{iso} = (\langle E_x^2 \rangle + \langle E_z^2 \rangle)/\langle E_y^2 \rangle$) leads to the same value. Also, Figure 8 shows the effect of the tilt angle on the ratio of the intensity of

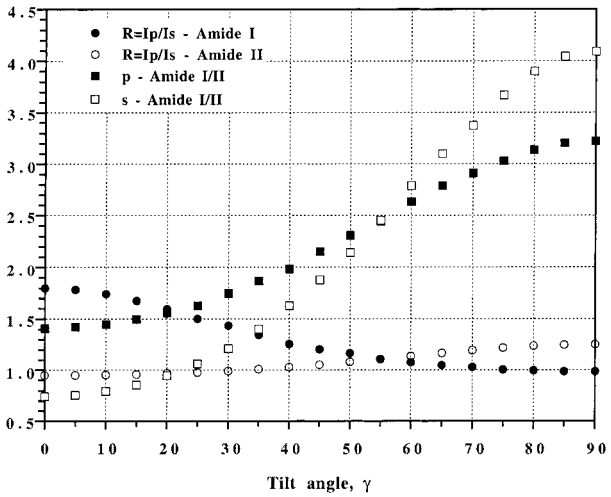

Figure 8. Influence of the tilt angle on the dichroic ratios of the amide I and amide II bands and on the ratio of the intensity of the amide I and amide II bands for the p and s polarizations.

the amide I and amide II bands ($R_{I/II}$), for the p and s polarizations. These parameters are more sensitive to the tilt angle than the dichroic ratios, in particular for high values of γ. This sensibility effect is more important for the polarization perpendicular to the plane of incidence. Thus, the $R_{I/II}$ parameter using s polarization could be used in the determination of the orientation of α-helices. This requires polarized ATR spectra with a sufficient signal-to-noise ratio in the spectral range of the amide II vibration.

Conclusion

Polarized ATR spectroscopy is a powerful method for studing the molecular orientation of thin films and in particular of α-helical polypeptides. Generally, the quantitative determination of the α-helices is obtained by calculating the molecular order parameter from the dichroic ratios of the amide I and amide II bands. This simple method requires an uniaxial orientation of the helices with respect to the normal of the surface and the knowledge of two main parameters: (i) the mean square electric field amplitudes of the evanescent polarized radiation in the film and, (ii) the orientation of the transition moment of the amide I and amide II modes with respect to the molecular axis. This study shows that these limitations can be overcome by using a spectral simulation approach. It consists of the determination of the anisotropic optical constants of the studied system, the simulation of the polarized ATR spectra for various orientations of the molecular axes, and the comparison of the simulated and experimental spectra. This approach has been applied to the orientation determination of the α-helices of PBG deposited on germanium crystal. Assuming that the α-helices are parallel to the plane of the ATR crystal, an azimuthal angle between the helix axes and the withdrawing direction of 38° ± 1° has been found. The influence of the azimuthal and tilt angles of the α-helices on the polarized ATR spectra has been investigated. The dichroic ratios of the amide I and amide II bands strongly vary with the azimuthal angle. Finally, these simulations show that the intensity ratio of amide I and amide II bands is more sensitive to the tilt angle than the dichroic ratio.

Acknowledgment. This work was supported in part by the Centre National de la Recherche Scientifique (CNRS, Département Sciences Chimiques), the Natural Sciences and Engineering Research Council of Canada (NSERC) and by the Fonds pour la Formation de Chercheurs et pour l'aide à la Recherche (Fonds FCAR) of the Province of Québec. I.P. is also grateful to NSERC and Fonds FCAR for postgraduate scholarships.

References and Notes

(1) Goormaghtigh, E.; Raussens, V.; Ruysschaert, J. M. *Biochim. Biophys. Acta* **1999**, *1422*, 105.
(2) Tamm, L. K.; Tatulian, S. A. *Q. Rev. Biophys.* **1997**, *30*, 365.
(3) Fringeli, U. P.; Günthard, H. H. Infrared Membrane Spectroscopy In *Membrane Spectroscopy*; Grell, E., Ed.; Springer-Verlag: New York, 1981, 270.
(4) Okamura, E.; Umemura, J.; Takenaka, T. *Biochim. Biophys. Acta* **1985**, *812*, 139.
(5) Ter-Minassian-Saraga, L.; Okamura, E.; Umemura, J.; Takenaka, T. *Biochim. Biophys. Acta* **1988**, *846*, 417.
(6) Lotta, T. I.; Laakkonen, L. J.; Virtanen, J. A.; Kinnunen, P. K. *Chem. Phys. Lipids* **1988**, *46*, 1.
(7) Okamura, E.; Umemura, J.; Takenaka, T. *Biochim. Biophys. Acta* **1990**, *1025*, 94.
(8) Hübner, W.; Mantch, H. H. *Biophys. J.* **1991**, *59*, 1261.
(9) Wenzl, P.; Fringeli, M.; Goette, J.; Fringeli, U. P. *Langmuir* **1994**, *10*, 4253.
(10) Lafrance, C. P.; Blochet, J. E.; Pézolet, M. *Biophys. J.* **1997**, *72*, 2559.
(11) Takenaka, T.; Harada, K.; Matsumoto, M. *J. Colloid Interface Sci.* **1980**, *73*, 569.
(12) Takeda, F.; Matsumoto, M.; Takenaka, T.; Fujiyoshi, Y. *J. Colloid Interface Sci.* **1981**, *84*, 220.
(13) Citra, M. J.; Axelsen, P. H. *Biophys. J.* **1996**, *71*, 1796.
(14) Okamura, E.; Umemura, J.; Takenaka, T. *Biochim. Biophys. Acta* **1986**, *856*, 68.
(15) Brauner, J. W.; Mendelsohn, R.; Prendergast, F. G. *Biochemistry* **1987**, *26*, 8151.
(16) Cornell, D. G.; Dluhy, R. A.; Briggs, M. S.; McKnight, C. J.; Gierash, L. M. *Biochemistry* **1989**, *28*, 2789.
(17) Fringeli, U. P.; Apell, H. J.; Fringeli, M.; Laüger, P. *Biochim. Biophys. Acta* **1989**, *984*, 301.
(18) Frey, S.; Tamm, L. K. *Biophys. J.* **1991**, *60*, 922.
(19) Subirade, M.; Salesse, C.; Marion, D.; Pézolet, M. *Biophys. J.* **1995**, *69*, 974.
(20) Axelsen, P. H.; Braddock, W. D.; Brokman, H. L.; Jones, C. M.; Dluhy, R. A.; Kaufman, B. K.; Puga, F. J., II *Appl. Spectrosc.* **1995**, *49*, 526.
(21) Axelsen, P. H.; Kaufman, B. K.; McElhaney, R. N.; Lewis, R. N. A. H. *Biophys. J.* **1995**, *69*, 2770.
(22) Lukes, P. J.; Petty, M. C.; Yarwood, J. *Langmuir* **1992**, *8*, 3043.
(23) Harrick, N. J. *J. Opt. Soc. Am.* **1965**, *55*, 851.
(24) Harrick, N. J. Internal Reflection Spectroscopy, Harrick Scientific Corporation, Ossining, New York **1967**.
(25) Hansen, W. H. *J. Opt. Soc. Am.* **1968**, *58*, 380.
(26) Axelsen, P. H.; Citra, M. *Prog. Biophys. Mol. Biol.* **1997**, *66*, 227.
(27) Higashiyama, T.; Takenaka, T. *J. Phys. Chem.* **1974**, *78*, 941.
(28) Jang, W. H.; Miller, J. D. *J. Phys. Chem.* **1995**, *99*, 10 272.
(29) American Institude of Physics Handbook; Gray, D. E., Ed.; McGraw-Hill: New York, 1972, Chapter 6.
(30) Handbook of Optics, Volume II; Bass, M., Ed.; McGraw-Hill: New York, 1995, Chapter 33.
(31) Bertie, J. E.; Amed, M. K.; Eysel, H. H. *J. Phys. Chem.* **1989**, *93*, 2210.
(32) Bertie, J. E.; Lan, Z. *Appl. Spectrosc.* **1996**, *50*, 1047.
(33) Rothschild, K. J.; Clark, N. A. *Biophys. J.* **1979**, *25*, 473.
(34) Nabedryk, E.; Breton, J. *Biochim. Biophys. Acta* **1981**, *635*, 515.
(35) Nabedryk, E.; Gingold, M. P.; Breton, J. *Biophys. J.* **1982**, *38*, 243.
(36) Buchet, R.; Varga, S.; Seidler, N. W.; Molnar, E.; Martonosi, A. *Biochim. Biophys. Acta* **1991**, *1068*, 201.
(37) Miyazawa, T.; Blout, E. R. *J. Am. Chem. Soc.* **1961**, *83*, 712.
(38) Tsuboi, M. *J. Polym. Sci.* **1962**, *59*, 139.
(39) Bradbury, E. M.; Brown, L.; Downie, A. R.; Elliott, A.; Fraser, R. D. B.; Hanby, W. E. *J. Mol. Biol.* **1962**, *5*, 230.
(40) Bazzi, M. D.; Woody, R. *Biophys. J.* **1985**, *48*, 957.
(41) Reisdorf, W. C., Jr.; Krimm, S. *Biophys. J.* **1995**, *69*, 271.
(42) Marsh, D.; Müller, M.; Schmitt, F. J. *Biophys. J.* **2000**, *78*, 2499.
(43) Marsh, D. *Biophys. J.* **1997**, *72*, 2710.
(44) Ahn, D. J.; Franses, E. I. *J. Phys. Chem.* **1992**, *96*, 9952.
(45) Ahn, D. J.; Franses, E. I. *Thin Solid Films* **1994**, *244*, 971.
(46) Buffeteau, T.; Blaudez, D.; Péré, E.; Desbat, B. *J. Phys. Chem. B* **1999**, *103*, 5020.
(47) Blaudez, D.; Boucher, F.; Buffeteau, T.; Desbat, B.; Grandbois, M.; Salesse, C. *Appl. Spectrosc.* **1999**, *53*, 1299.
(48) Picard, F.; Buffeteau, T.; Desbat, B.; Auger, M.; Pézolet, M. *Biophys. J.* **1999**, *76*, 539.

(49) Buffeteau, T.; Le Calvez, E.; Castano, S.; Desbat, B.; Blaudez, D.; Dufourcq, J. *J. Phys. Chem. B*, **2000**, *104*, 4537.
(50) Loeb, G. I. *J. Colloid Interface Sci.* **1968**, *26*, 236.
(51) Lavigne, P.; Tancrède, P.; Lamarche, F.; Grandbois, M.; Salesse, C. *Thin Solid Films* **1994**, *242*, 229.
(52) Fukuto, M.; Heilmann, R. K.; Pershan, P. S.; Yu, S. M.; Griffiths, J. A.; Tirrell, D. A. *J. Chem. Phys.* **1999**, *111*, 9761.
(53) Berreman, D. W. *J. Opt. Soc. Am.* **1972**, *62*, 502.
(54) Azzam, R. M. A.; Bashara, N. M. *Ellipsometry and Polarized Light*; North-Holland: Amsterdam, 1977, Chapter 4.
(55) Graybeal, J. D. *Molecular Spectroscopy*; McGraw-Hill, Inc.: New York, 1988; p 665.
(56) Miyazawa, T. *Poly-α-amino Acids*; Fasman, G. D., Ed.; Marcel Dekker: New York, 1967; Chapter 2, 69−103.